XLIII CILAMCE
21–25, November, 2022
FOZ DO IGUAÇU – PR – BRAZIL

Numerical Simulation of the Deep Stamping Process

Gabriel Guimarães Hofmam[1], Valter Alvares Gonzaga Filho[1], Lúcio Starling de Azevedo[1], Matheus Correa Santos[1], Brenda Kennedy de Oliveira[1], Lucival Malcher[1].

[1]*Dept. of Mechanical Engineering, University of Brasilia*
UnB, 70297-400, DF/Brasília, Brazil
malcher@unb.br, 170058212@aluno.unb.br

Abstract. The process of stamping is largely used when manufacturing a variety of structural and mechanical components, composed basically of a die, a punch, and a blank holder. The CAE finite elements software, Abaqus, allows the modeling, simulation, and analysis of the stamping process thus showing the influence the punch displacement speed has over the maximum stress in the material. By the end of the analysis, including mesh convergence studies, it is easy to observe that greater speeds result in greater stress levels of the workpiece and larger deformations of its intended geometry. The study found that optimal punch speed levels for manufacturing small aluminum cups lie between ranges of 40 to 60 mm/s.

Keywords: Deep stamp, numerical simulation, speed analysis

1 Introduction

Stamping is a manufacturing process that produces the end geometry through shearing or deformation of sheet metal plates by pressing them with a punch into a die. As presented by Groover [1], three main types of stamping are used in sheet metal working: bending stamping, where geometries are formed by pushing the sheet onto a matrix which bends it to the designated shape, shearing stamping, where the punch cuts a blank from the starting coil, and deep drawn stamping, where the die consists of a deep cylindrical surface resulting in end pieces having a tube-like structure, such as a pressure cooker. This work focuses on analyzing the effect of die speed on an application of the former stamping method for forming small aluminum cups, by way of numerical simulations through Finite Element Analysis (FEA). Results achieved have then enabled considerations on model stability, fracture, end-piece shape integrity and effects on expected power usage during manufacturing

1.1 Overview of the deep-drawn stamping process

Deep-drawn stamping processes require the use of tools such as the ones represented onFigure 1.

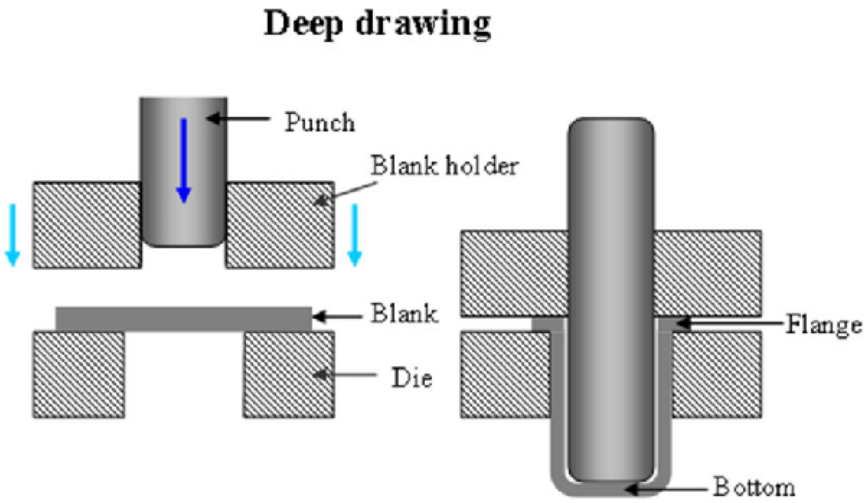

Figure 1. Tools used in deep-drawn stamping processes.
Font: Reproduction/Hosseini, Ebrahimi-Mamaghani, and Asa [2]

As illustrated in Figure 1, deep-drawn stamping components consist of a die, a punch, a blank and a blank holder. The die defines the end shape of the piece, while the die is used for applying downward pressure on the blank. The blank holder ensures that the workpiece does not slide off-center during the process.

Sheet metal working is a simple manufacturing process that offer some advantageous characteristics, such as:

- High output rate;
- Reduced cost per unit produced;
- Reasonable surface finish.

2 Starting Parameters and Problem Assembly

Simulations were made using Abaqus 2020, a commercial FEA package. Modeling of the problem utilized a Dynamic-Explicit FEA model and applied an axisymmetric approximation for representing its components. For the sake of simplicity and performance, thermodynamic effects, friction and damage models, and other parameters of lesser impact, were omitted from the analysis.

Aluminum (Al 6101) was chosen as the sheet material for the circular blank, which is 40 mm large and 2 mm deep. The elastic properties of the material are as shown in Table 1.

Table 1. Al6101 elastic properties

Elasticity Modulus	**Poisson's Coefficient**
E = 70 GPa	ν = 0,3

Regarding the plastic properties, they were drawn from the isotropic hardening curve yielded by experiments performed by **Autor**, obtained from the equation.

$$\delta_y = \delta_{y_0} + H \cdot \varepsilon^{-p^n} \tag{1}$$

Where $\delta_{y_0} = 96$, $H = 192.6$, $n = 0.349$ and ε^{-p^n} vary from 0 to 1.5 with an increment of 0.01 from 0.0 to 0.1, increment of 0.05 form 0.1 to 0.3 and an increment of 0.1 from 0.3 to 1.5.

Since it is an explicit simulation, the density becomes relevant, as the inertial forces must be calculated. The density of the aluminum used is $0.0027 g/mm^3$.

The problem model was thus assembled in accordance to Figure 2.

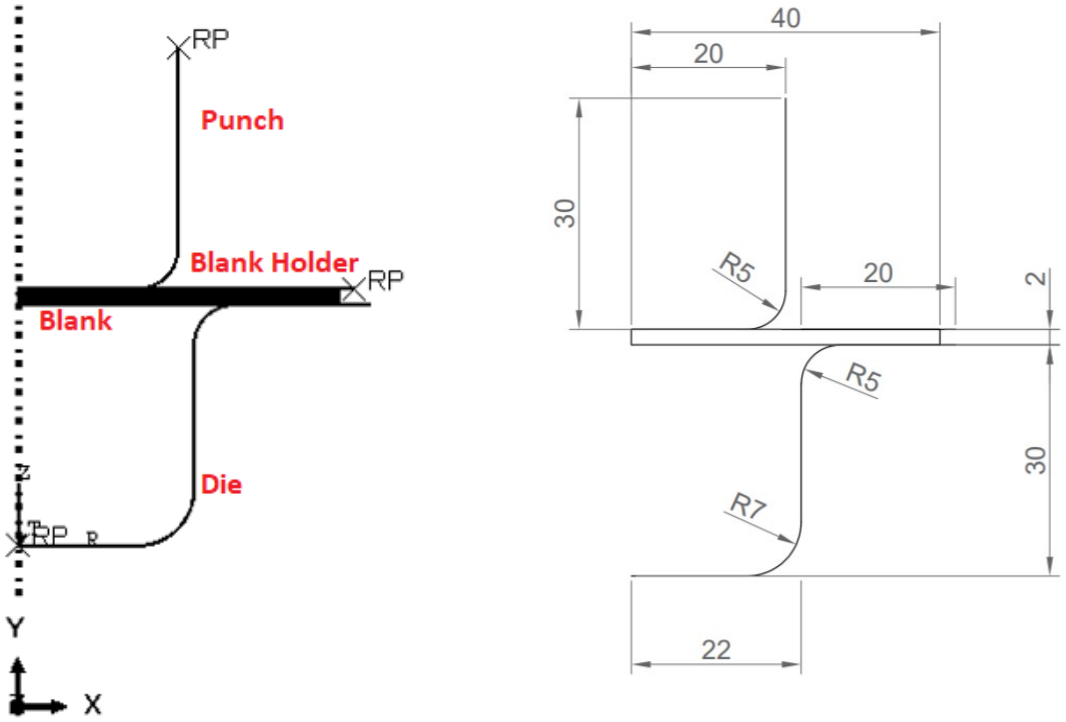

(a) Assembly. (b) Dimensions.

Figure 2. Dimensional Parameters.

In regards to the interactions, surface-to-surface contact was defined between the punch and blank, the die and blank and between the blank and blank holder. Normal contact was defined as strong contact and tangential contact as frictionless.

In this simulation, the blank holder, punch and die were considered as rigid bodies. Thus, the following boundary conditions were applied to the reference points (RP) coupled to them:

- Encastre of the blank holder and die in the initial step;
- Restrictions of the displacement on the x-axis and of the rotation around the z-axis of the punch;
- y-axis displacement of the punch by 30 mm, towards the die, in the following step. Time from standstill to maximum travel was set as the time amplitude of this boundary condition, therefore controlling the punch's speed.

The reaction force applied by the deforming sheet metal on the punch was then recorded by the program, as measured on the component's reference point.

Considering the dynamic nature of this simulation, speed is a variable of utmost interest. To this effect, a linear increment in displacement from the punch at standstill to it's max travel value, at 30 mm was defined. In addition, the total time for the process was set at multiple values, each evaluated separately, alternating between 0.25, 0.50, 0.75, 1.00, 1.50 and 2.00 seconds. Hence, resulting travel speeds of the punch of 120, 60, 40, 30, 20 and 15 mm/s were achieved and studied.

3 METHODOLOGY

The methodology used to show the effects of the travel speed of the punch on the stamping process is as follows:

- Establish mesh convergence and define the optimal number of nodes (refinement degree and element type) to be used during the simulations;
- From the initial speed of 30mm/s, come up with a range of values for the speed to be analyzed;
- Verify the effects speed has on the Von Mises stress, the force applied, and the plastic strain;

The mesh convergence analysis was performed with quadrilateral linear elements. It was possible to verify a convergence zone in the region of elements sizes between 0.5 and 0.1 mm. The values obtained from the mesh

convergence study are listed in Table 2.

3.1 Mesh Convergence Analyses

As shown in Table 2, the convergence study for the 10 meshes analyzed resulted in a sequence of values for the equivalent von Mises stress with small variations between each, equivalent to 3 hundredths to a thousandth of a unit, even for large increments in the level of refinement.

Table 2. Mesh Convergence Data

Element Type	σ_{vm} [MPa]	Discretization	Number of Nodes	$\Delta\sigma_{vm}/N_{nodes}$
Linear quadrilateral	262,0	1,0	123	-
Linear quadrilateral	261,6	0,9	135	-0,0333
Linear quadrilateral	262,3	0,8	204	0,0101
Linear quadrilateral	264,3	0,7	232	0,0714
Linear quadrilateral	263,8	0,6	272	-0,0125
Linear quadrilateral	265,7	0,5	405	0,0143
Linear quadrilateral	265,9	0,4	606	0,0010
Linear quadrilateral	266,3	0,3	1072	0,0009
Linear quadrilateral	267,0	0,2	2211	0,0006
Linear quadrilateral	272,3	0,1	8421	0,0009

Crafted from the data presented in Table 2, the graph from Figure 3 allows the assessment of the equivalent Mises stress as a function of the number of nodes.

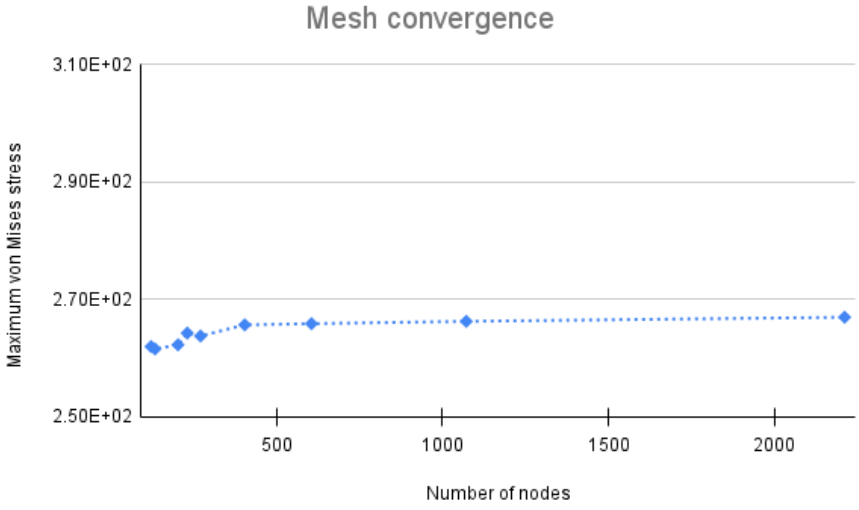

Figure 3. Mesh convergence graph

Based on the graph,Figure 3, it is possible to observe that from a global element size of 0.5 onward, there is an acceptable convergence of the stress values. Therefore, this value for the mesh element size was considered to yield an optimal balance between accuracy for the resulting part stress and required computational times.

The following speeds were then set, starting from the initial speed of 15 mm/s and ranging to 120mm/s, encompassing intermediate values of 20 mm/s, 30 mm/s, 40 mm/s, and 60 mm/s, by way of the methodology specified in section 2.

Results yielded by Abaqus for the variables of interest were then processed and studied.

4 RESULTS

4.1 Stress and Strain as a function of speed

As per the results presented in Figure 4, the force required to deform the blank applied to the punch at each instant in time follows a similar profile for each forward speed evaluated.

Although the energy used in the process remains almost unchanged since the displacement is fixed and the instantaneous force has minimal variation, power consumption in the process changes with speed variations. Manufacturing performed at higher speeds implies greater power dissipation, a relevant consideration due to the possibility of heating both tool and workpiece, as well as the need for machinery with greater power output.

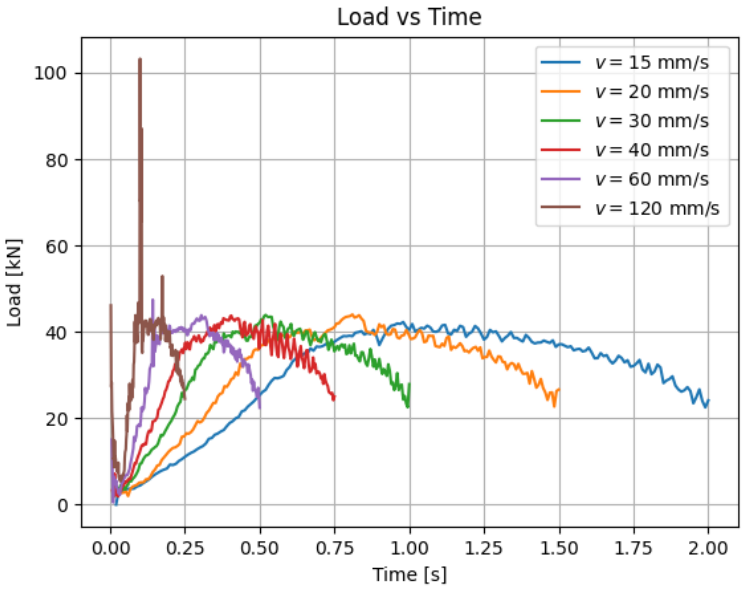

Figure 4. Force as a Function of Time

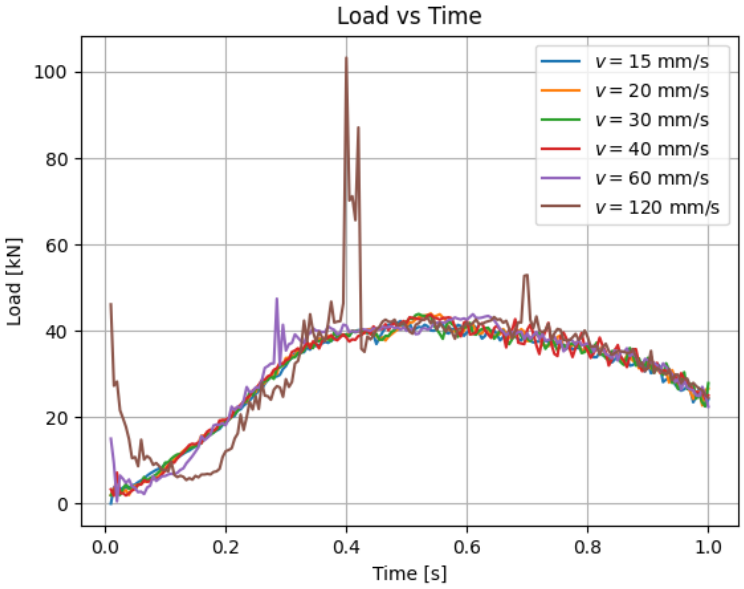

Figure 5. Force as a Function of Characteristic Time

Through the information presented in the graph, it is possible to infer that: simulations with higher punch displacement speed, above 40 mm/s, have higher instability compared to those with lower speed. This results in a

distortion of the part geometry, as can be seen in Figure 6. Therefore, a speed of 60 mm/s is found to optimally balance the manufacturing time and quality of the manufactured part, presenting but minimal anomalies.

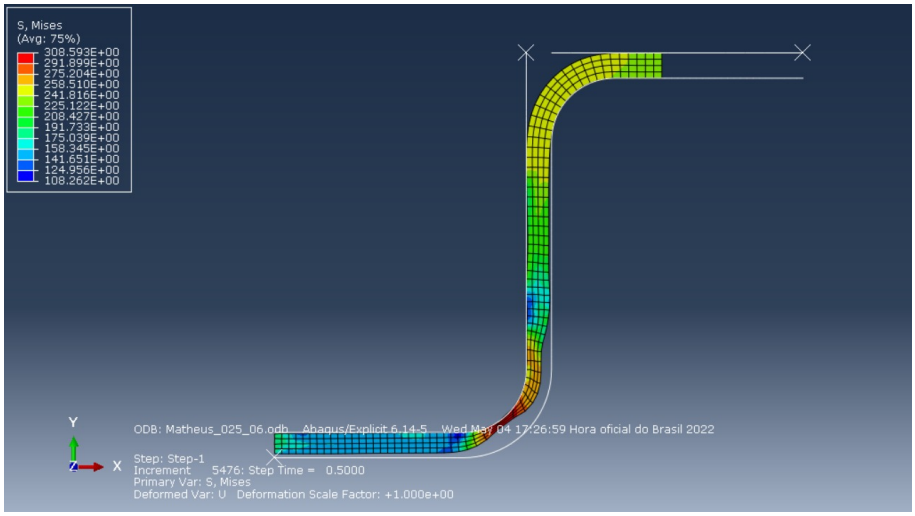

Figure 6. 0.5 mesh with 0.5 time-step

For especially high speeds, specifically 120 mm/s, it is still possible to identify erratic behavior in the distribution of stresses and strains in the mesh, illustrated in Figure 7. This anomaly is also observed in the force-by-time plot from Figure 4, where there is a peak in the stress readings which bears no physical meaning.

(a) Von Mises stress, t=0.25s

(b) Equivalent Strain, t=0.25s

Figure 7. Simulation Results

The results of the equivalent von Mises stress and strain, provided by the simulation with 40 mm/s speed, follow, respectively, the distribution pattern shown in Figures 8 and 9

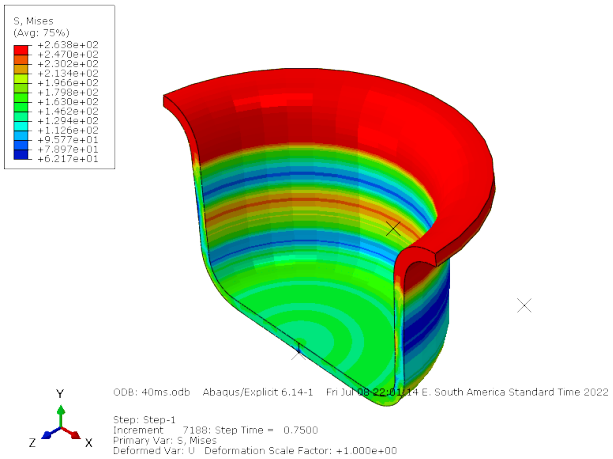

Figure 8. Von Mises stress for speed 40 mm/s

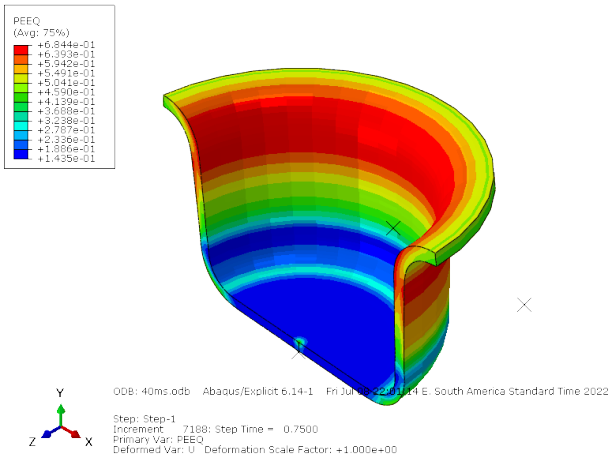

Figure 9. Strain for speed 40 mm/s

The stress and strain values obtained for each speed level were listed in Table 3.

Time [s]	MAX(σ_{vm}) [MPa]	Deformation	Speed [mm/s]
2	265,5	0,7191	15
1,5	265,8	0,7122	20
1	265,8	0,7106	30
0,5	308,6	1,407	60
0,25	313,2	1,52	120

Table 3. Table of characteristics by time

The stress distribution indicates large concentrations at the top edge of the component, which configures the critical point where possible failures can occur. The plots in Figures 10 and 11 show an increase in stress and strain levels as a function of the speed increment.

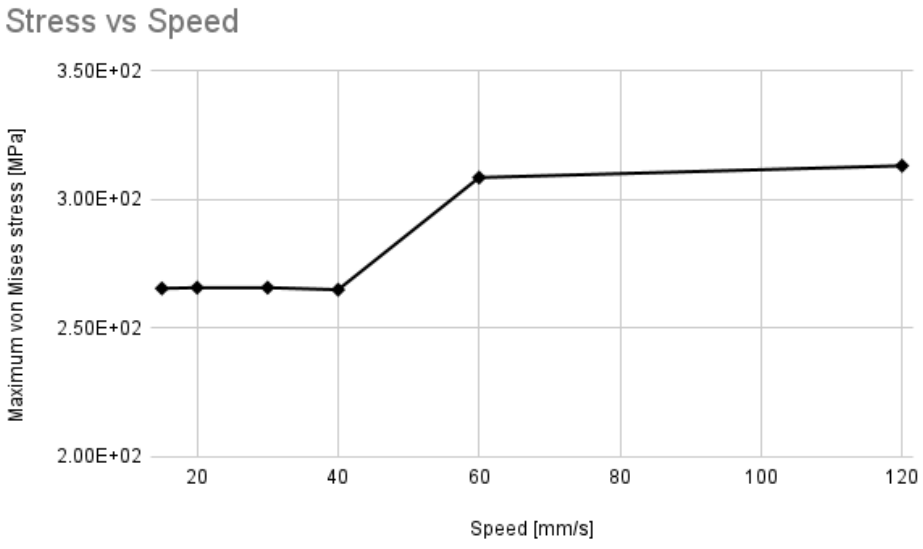

Figure 10. Stress as a Function of Speed

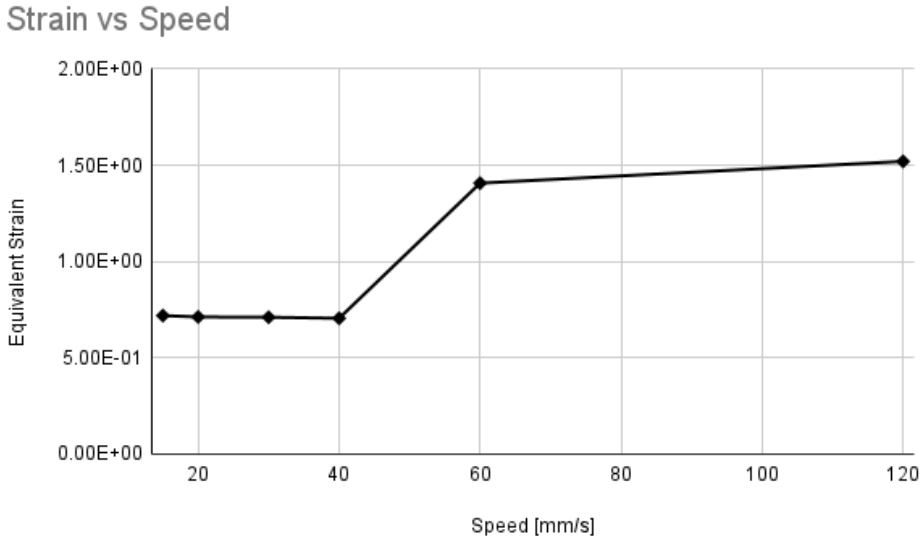

Figure 11. Strain as a Function of Speed

5 Conclusions

In industrial applications, manufacturing speed is a defining factor when it comes to productivity, directly affecting profit margins and the ability to quell surges in demand. However, during the analysis made it became clear that, for increased punch velocities, the object presents excessive stress, greater deformation levels, and loads with abrupt variations. Thereby is expected that there is an optimal speed that grants both sufficient endpiece quality and productivity. As such, this study found a punch speed of 60mm/s to yield reasonable results in both these metrics.

Considering the relatively sizeable step used in this study, measuring roughly 20 mm/s per increment, a more in deep study of the speed between 40mm/s and 60mm/s is suggested for future developments. Further considerations are the modeling of friction and other simulation parameters to find a more accurate approximation for the maximum speed which does not result in loss of the object geometry.

Acknowledgements. The authors acknowledge the support of the University of Brasilia - UnB and the National Council for Scientific and Technological Development - CNPq.

Authorship statement. The authors hereby confirm that they are the sole liable persons responsible for the authorship of this work, and that all material that has been herein included as part of the present paper is either the property (and authorship) of the authors, or has the permission of the owners to be included here.

Bibliography

[1] Mikell P. Groover. *Fundamentals of Modern Manufacturing: Materials, Processes, and Systems*. John Wiley & Sons, Jan. 7, 2010. 1027 pp. ISBN: 978-0-470-46700-8.

[2] Rouhollah Hosseini, Ali Ebrahimi-Mamaghani, and Alireza Asa. *An Investigation Into the Effects of Friction and Anisotropy Coefficients and Work Hardening Exponent on Deep Drawing with FEM*. Jan. 20, 2013.